



UNCERTAINTIES IN DETERMINING DIAPHRAGM FLEXIBILITY

K.T. TOKORO¹, J.C. ANDERSON² and V.V. BERTERO³

SUMMARY

Concrete roof and floor slabs deflect negligibly under the action of in-plane loading and are classified as rigid diaphragms, whereas wood diaphragms can deform more and are classified as either rigid or flexible diaphragms. The flexibility of the diaphragm can have a significant effect on the distribution of horizontal diaphragm forces to the vertical elements (shearwalls) that transfer these forces to the foundation. A significant increase in the anchorage forces between the diaphragm and either concrete or masonry walls are also required for flexible diaphragms. Current practice is to consider all wood diaphragms as flexible. Although several building codes have specific criteria for diaphragm classification, considerable ambiguity exists in the application and interpretation of these criteria.

The purpose of this paper is to investigate some of the uncertainties that arise in the application of current code criteria for flexible or rigid diaphragms. An instrumented three story building with masonry shearwalls and wood diaphragms will be considered for study. This building has been instrumented with 13 seismic sensors and has recorded response data from several earthquakes including Whittier Narrows (1987), Landers (1992) and Northridge (1994). A three dimensional finite element model of this building was developed for analysis in both principal directions using the ETABS computer program. Criteria for classifying the diaphragms of this building as flexible or rigid will be investigated using the static equivalent lateral loads specified in current building codes, followed by a detailed analysis of the recorded data and its implications for rigid versus flexible design criteria. Gaps in the recorded data will be identified and the recorded response will be supplemented by conducting dynamic analyses using the base motions recorded during the Landers earthquake. Finally, the flexibility of the diaphragms will be evaluated in terms of the horizontal force distributions to the vertical elements (shearwalls).

INTRODUCTION

Observed damage following moderate to large earthquakes has shown that masonry buildings are vulnerable to lateral shaking [1]. Fallen brick and mortar constitute a life-safety hazard that must be mitigated for future earthquakes. The two most important methods to prevent damage, destruction and loss of life are to constantly improve the current standards by which buildings are designed, as well as to

¹ Graduate Student, Stanford University, Stanford, USA. Email: tokoro@stanford.edu

² Professor, University of Southern California, Los Angeles, USA. Email: jamesa@usc.edu

³ Professor Emeritus, University of California, Berkeley, USA. Email: vbertero@aol.com

focus on developing effective methods for the rehabilitation and/or upgrading of buildings which have been shown to be vulnerable to lateral shaking.

Few experimental research studies have attempted to assess the dynamic response of masonry structures with wood diaphragms. An alternative to using either full-scale or reduced-scale experiments to evaluate the dynamic response of this class of buildings is to develop analytical models that can be shown to closely emulate the response obtained from instrumented buildings for which there is recorded acceleration data.

Structures with flexible floor diaphragms behave intrinsically different under dynamic lateral loading than structures with rigid diaphragms. This has been recognized by building codes, including the 1997 Uniform Building Code (UBC) in section 1633.2.9, which specify provisions for the seismic design of newly constructed building systems considering flexible-diaphragm behavior [2]. However, a clear criterion for determining when a diaphragm is flexible or rigid is not available for application in practice. Flexible-diaphragm systems continue to be analyzed using the same criteria and recommendations as developed for structures with rigid diaphragms, which may not necessarily be a conservative approach. Research has shown that structures with flexible diaphragms may experience higher accelerations and displacements than structures with rigid diaphragms, and their fundamental periods of vibration may be significantly longer [3].

Although it is known that properly detailed, reinforced masonry buildings can develop sufficient stiffness and strength, their seismic performance has not been well documented in the past. Therefore, the seismic behavior of masonry structures is still not completely understood. Certain masonry structures have performed well when subjected to strong ground motion and modern masonry construction has also had a satisfactory performance in recent earthquakes. Of the buildings with such modern characteristics is a three-story office building in Lancaster, California. This building is of particular interest for analytical studies as it is among the few reinforced masonry buildings that have been instrumented by the California Strong Motion Instrumentation Program (CSMIP). Although a significant amplification of the peak ground acceleration was observed at the roof level, the building had satisfactory performance despite the intensity of the seismic shaking. The analytical study of the performance of this building serves as a means for enhancing our understanding of how similar masonry structures may respond when subjected to moderate and strong ground motions.

EXAMPLE STRUCTURE AND GROUND MOTIONS

Building Description

An instrumented three-story building that was designed in 1975 is used as the subject of this investigation. The building has a rectangular plan that is 72' x 129' and a total height of 37.5'. A simplified plan view showing the structural components of a typical floor is presented in **Figure 1**. The building is rectangular in shape, with the exception of the two rectangular stairwells located at the north and south ends of the building. The longitudinal dimension of the building is aligned in a North-South direction. The lateral force resisting system is composed of grouted concrete masonry unit block walls in the N-S and E-W directions together with plywood diaphragm floor systems. In addition to the masonry walls, vertical loads are also supported by rectangular steel tube columns located on interior and exterior column lines having an equal number in each story of the building. The building foundation consists of concrete piers.

Diaphragms

The roof diaphragm of the three-story office building in Lancaster consists of 4' x 8' x 1/2" thick structural I plywood mounted on 20" TJI truss joists running in the E-W direction at 24" o.c., while plywood edges were nailed to 2x4 Douglas Fir studs at 48" o.c. in the N-S direction. The second and third floor diaphragms consisted of 1 1/8" Structural I plywood mounted on 30" TJI open web truss joists at every 24" o.c. in the E-W direction, and on 2x4 Douglas Fir studs in the N-S direction.

Grouted walls

The walls of the building are 8" and 12" grouted Concrete Masonry Unit block walls. The primary lateral force resisting system in the N-S direction consists of four 12" walls located four feet on either side of the N-S centerline of the building. Three 8" walls were used in the E-W direction for lateral resistance with one at the N-S centerline and one at each end. Typical vertical and horizontal reinforcing in the 8" walls consisted of 1-#5 bar spaced at 32" o.c. and 1-#4 bar spaced at 24" o.c. The 12" walls contained 2-#4 bars spaced at 24" o.c. horizontally, while 2-#4 bars spaced at 32" were used as vertical reinforcement.

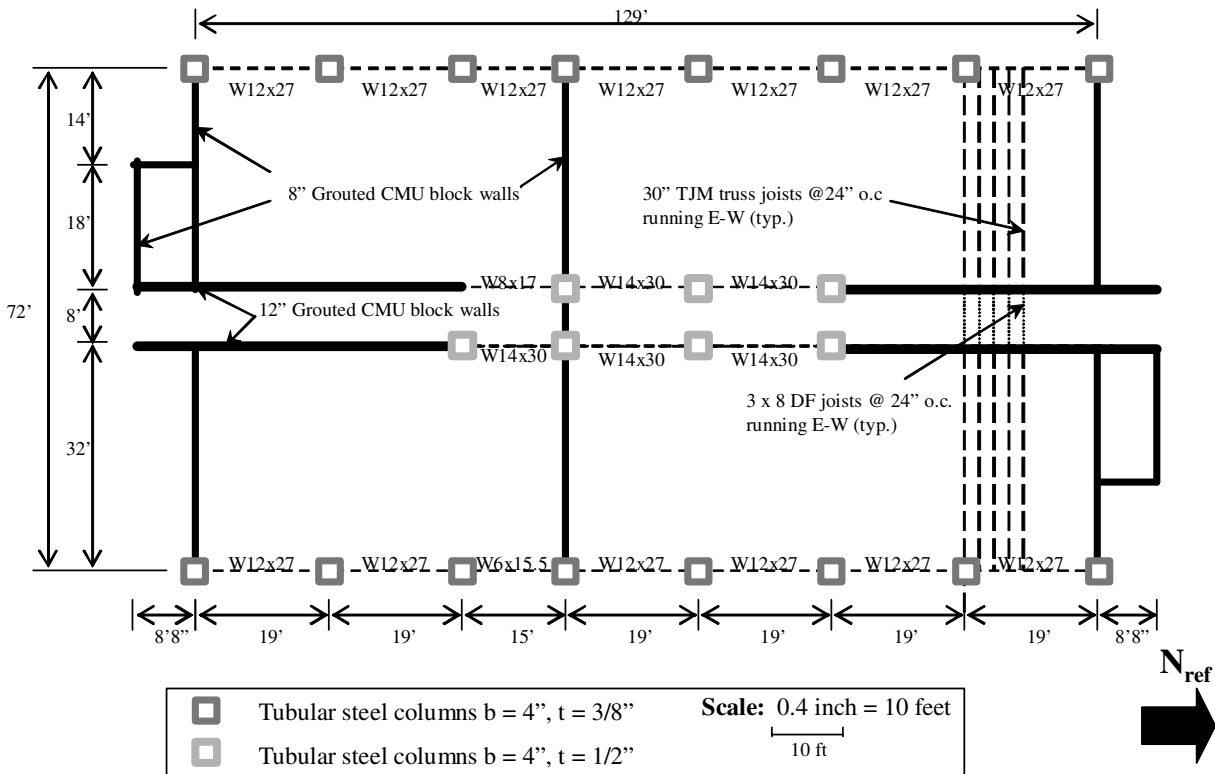


Figure 1. Typical plan view, 3-story building.

Instrumentation and Recorded Response

The California Strong Motion Instrumentation Program (CSMIP) instrumented the three-story office building with thirteen sensors [4]. The location of each sensor is shown schematically in **Figure 2**. Sensors 1, 9 and 13 recorded motions at the base. Sensors 8 and 12 recorded horizontal accelerations at the second floor level. Sensors 5, 6, 7, and 11 recorded horizontal accelerations at the third floor level, and sensors 2, 3, 4 and 10 measured the horizontal accelerations of the roof during the earthquakes. Acceleration data recorded at each of the 13 channels were available from CSMIP. Though recorded response data for the three-story building was available for the Whittier Narrows (1987), Landers (1992) and Northridge (1994) earthquakes, only the Landers ground motion was used for analytical investigation because it corresponded to the peak acceleration at the base of the three-story building in the E-W direction.

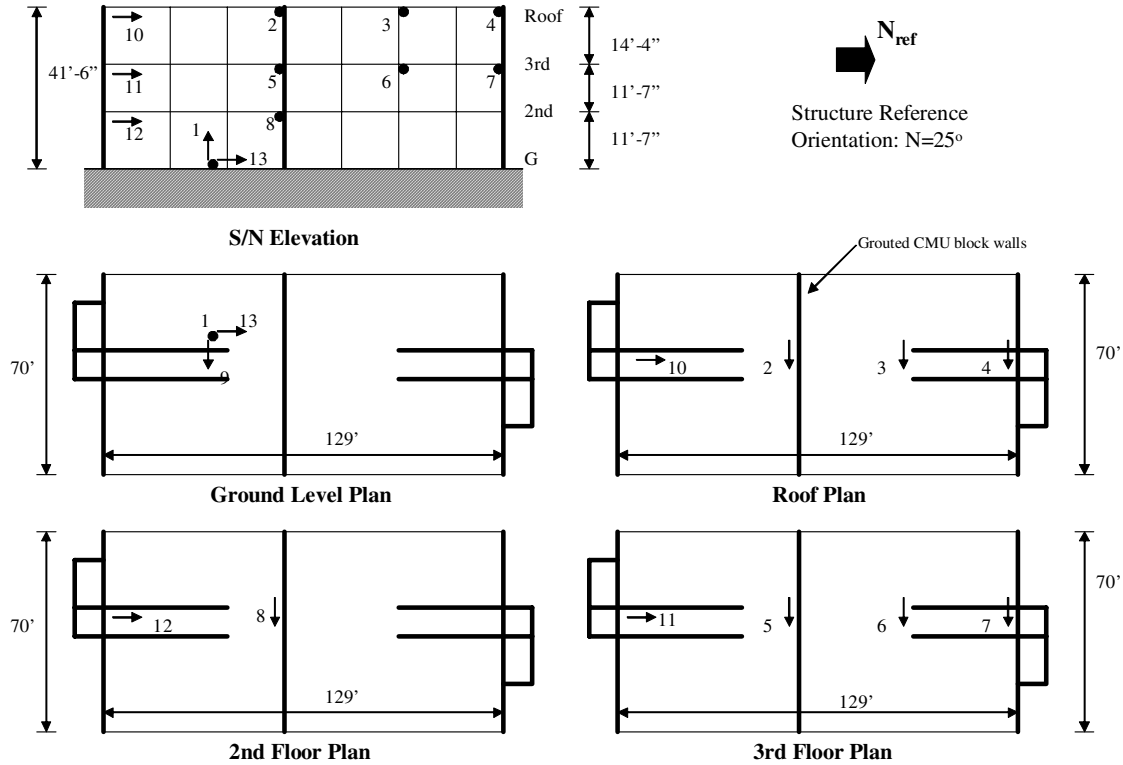


Figure 2. Location of strong motion instrumentation.

Recorded Motions During the Landers Earthquake (1992)

The time histories showing the recorded accelerations and displacements at each of the 13 sensors during the Landers earthquake are shown elsewhere [5]. During the Landers Earthquake, the sensors recorded a total of 80 seconds of acceleration data, although only 7 seconds were considered to be significant ground motion. Peak accelerations recorded for each sensor during the Landers earthquake are summarized in **Table 1**. Response Spectra for the recorded N-S and E-W base motions during the Landers earthquake are shown in **Figure 3**.

Table 1. Peak recorded accelerations.

Sensor I.D.	Location	Peak Absolute Acceleration (g)		
		Whittier Narrows	Landers	Northridge
1	Ground (UP)	0.02	0.04	0.04
2	Roof (E-W)	0.09	0.09	0.07
3	Roof (E-W)	0.18	0.24	0.12
4	Roof (E-W)	0.07	0.09	0.07
5	3RD (E-W)	0.08	0.09	0.06
6	3RD (E-W)	0.15	0.19	0.13
7	3RD (E-W)	0.07	0.09	0.06
8	2ND (E-W)	0.06	0.07	0.05
9	Ground (E-W)	0.06	0.07	0.04
10	Roof (N-S)	0.06	0.06	0.09
11	3RD (N-S)	0.05	0.05	0.08
12	2ND (N-S)	0.05	0.04	0.07
13	Ground (N-S)	0.04	0.04	0.07

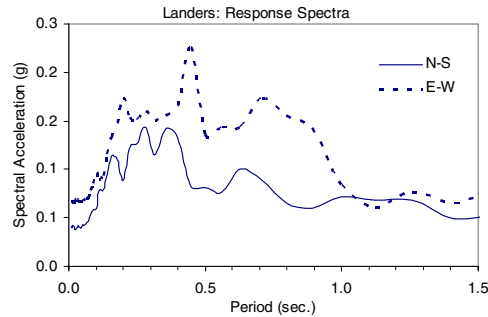


Figure 3. N-S and E-W response spectra, Landers.

An inspection of the acceleration and displacement time histories indicates that the frequency of the accelerations and displacements for each channel stay relatively constant even following the strongest portion of the base motion. Such a result suggests that the building responded in an essentially elastic manner during the Landers earthquake.

Amplification of the peak acceleration between the ground and roof levels was observed in the E-W direction during the Landers earthquake, due to the in-plane flexibility of the diaphragms in the transverse building direction. During the Landers earthquake, the middle wall of the E-W lateral force resisting system experienced a peak roof acceleration of 0.09g as measured by sensor 2, while a peak roof acceleration of 0.24g was experienced midway between the middle and north walls as measured by sensor 3. However, the peak ground acceleration in the E-W direction during the Landers Earthquake was only 0.07g as measured by sensor 9. The recorded data shows that only slight amplification of the peak acceleration between the ground and roof occurred in the N-S direction. A peak acceleration of 0.06g at the roof level as measured by sensor 10, whereas the peak N-S ground acceleration as measured by sensor 13 was 0.04g. However, no instrument was located near the edge of the roof diaphragm where amplification may have occurred. The peak vertical ground acceleration of the three-story building during the Landers earthquake was 0.04g, which is not considered to be significant.

METHODOLOGY

Elastic Dynamic Analyses/Mathematical Model

Three-dimensional dynamic analyses of building structures have traditionally not been done because of high computational demands and memory requirements. However, with the surge in computational capabilities available to engineering offices, such analyses may be used for more conventional structural systems. A wide variety of general-purpose computer software is currently available for the static and dynamic structural analysis of complex frame structures. Most of these programs can be used for the analysis of multistory frame and shear wall buildings. However, ETABS [6] is a special purpose computer program developed specifically for building systems. It has simplified input and output that reduces the time required for development of the analytical model and the time to evaluate the final results. This finite element based software package has been in development since the late 60's, and has proven to be an invaluable design and analysis aid to structural engineers.

Although masonry is known to be a highly nonlinear material, Moving Window Fourier Transfer Function analyses of time history data recording in the building during each of the three earthquakes indicated that the building remained essentially elastic during all three earthquakes. Therefore, it was deemed sufficient to develop a linear model to evaluate the dynamic response. Due to the expected interaction of the walls, base slab and diaphragms, a three-dimensional linear elastic finite element model of the three-story building was developed using ETABS (Version 7) computer software, though it is

recognized that other computer programs could have been used. An isometric view of the 3-D linear elastic analytical model of the three-story building is shown in **Figure 4**. The model consists of a total of 5,112 nodal points. To accurately reproduce the flexibility of the diaphragms, 6,413 shell elements were used, which is well above the recommended minimum [6]. The columns, edge beams and interior beams were modeled using 824 frame elements.

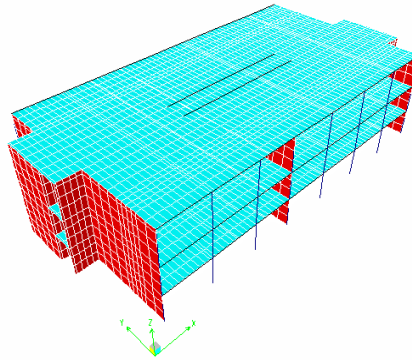


Figure 4. 3-D linear elastic ETABS model, isometric view.

Diaphragm Flexibility

It is of interest to investigate the UBC 1997 requirements for diaphragm flexibility as applied to the three-story building. The UBC 1997 code requirement will be computed for the three-story building using both static and dynamic loading cases, and the suitability of these requirements will be discussed.

1997 UBC Flexible Diaphragm Requirement

Section 1630.6 of the 1997 Uniform Building Code states that “Diaphragms shall be considered flexible for the purposes of distribution of story shear and torsional moment when the maximum lateral deformation of the diaphragm is more than two times the average story drift of the associated story.” Thus, the code condition may be expressed using **Equation (1)**. This ratio can be determined as the lateral in-plane displacement of the diaphragm itself under lateral load relative to the story drift of adjoining vertical-resisting elements (walls) under equivalent tributary lateral load. It should also be noted that “story drift” is the lateral displacement of one level relative to the level above or below.

$$1997\text{UBC} : \frac{\text{maximum lateral deformation of diaphragm.}}{\text{average associated story drift}} > 2 \quad (1)$$

1997 UBC Flexible Diaphragm Verification

Verification of diaphragm flexibility was conducted by comparison of the mid-span relative deflection and corresponding support displacement of the roof and 3rd floor diaphragms of the 3-story building in the N-S and E-W building directions. Displacement time history results for the desired locations along the diaphragm were obtained using the ETABS linear elastic mathematical model subjected to the recorded base motions during the Landers earthquake. As previously mentioned, the maximum base acceleration recorded during the three earthquakes for which there are recorded data was 0.07g (Landers), thus it was deemed appropriate to limit this part of the study to characterize the flexibility of the roof and 3rd floor diaphragms based on the displacement response of the building during the Landers earthquake.

Separate flexibility analyses were conducted using both static equivalent lateral loads as per 1997 UBC, and using dynamic time history analysis results. It should be noted that the 1997 UBC requirement for considering a diaphragm as flexible is for analysis and design using the static procedure and loading the structure independently in each of the two principal directions.

The steps taken to compute the ratio for this study will be discussed in this section. The calculations performed for the 1997 UBC displacement ratio for flexible diaphragm verification are illustrated in **Figures 5 and 6**. Note that this figure is not meant to represent the actual configuration of any of the buildings considered in this study. Also, for the sake of simplicity, the drawings shown represent the case where no torsion is present. The grey lines in the diagram represent the undeformed configuration, and the black lines represent the assumed deformed configuration resulting from seismic loading. The steps required to compute the numerator of the 1997 UBC ratio (level i) for this example building are illustrated in **Figure 5**. The maximum diaphragm deformation is the displacement at midspan (relative to the base) for the level of the building under consideration (i.e. level i) minus the average displacements (relative to the base) at the vertical supports. Computation of the denominator for the 1997 UBC displacement ratio is illustrated in **Figure 6**. The denominator requires computation of the interstory drift, which considers the displacement of the story below the level of interest (i.e. $j = i - 1$). The interstory drift for story j is computed for each vertical support and these two values of interstory drift are averaged to obtain the resulting denominator for the 1997 UBC displacement ratio for story j . Hence the displacement ratio becomes Δ_{\max}/δ_0 .

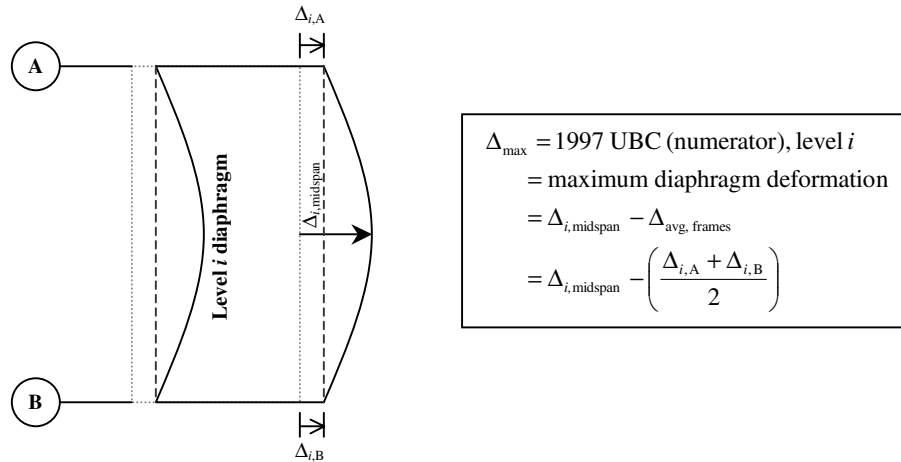


Figure 5. Example calculation of numerator, 1997 UBC ratio.

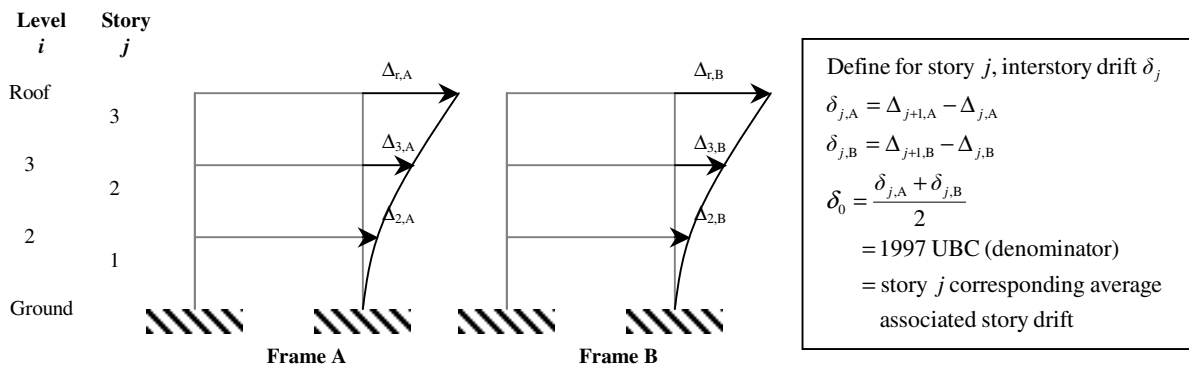


Figure 6. Example calculation of denominator, 1997 UBC ratio.

Static Loading

Diaphragm flexibility under static loading was studied by considering the behavior of the three-story building under the 1997 UBC inverted triangular static equivalent lateral load pattern were applied separately in the N-S and E-W building direction. The load patterns used were generated with the ETABS 1997 UBC automatic lateral load generating option, and were applied to the building through its center of mass parallel to the N-S and E-W building directions.

Diaphragm flexibility was considered for both directions. To compute the displacement ratio to be compared to the 1997 UBC code criteria for the E-W direction, the maximum lateral deformation of the sub-diaphragm was taken to be the difference between the maximum displacement along the sub-diaphragm between the adjacent supports and the average displacement of the two adjacent supports. For the N-S direction, maximum lateral deformation in the diaphragm was the difference between the deformation at the “unsupported” edge of the sub-diaphragm and the deformation of the supporting walls. Additionally, for either direction, the “average associated story drift” was taken as the average interstory drift of the vertical resisting elements (walls) associated with the sub-diaphragm.

In order to calculate numeric ratios for comparison using the ETABS analytical results, it was necessary to compute the ratios using defined points along the wall and diaphragm near the instrument locations. It was necessary to add two supplemental points at the edge of the diaphragm as indicated by A and B. The points for ratio calculation are shown as a schematic diagram of the plan views of the roof and 3rd floors of the building in **Figure 7**. For convenience, the walls of the building oriented in the E-W direction are labeled from left to right as W1, W2 and W3, respectively.

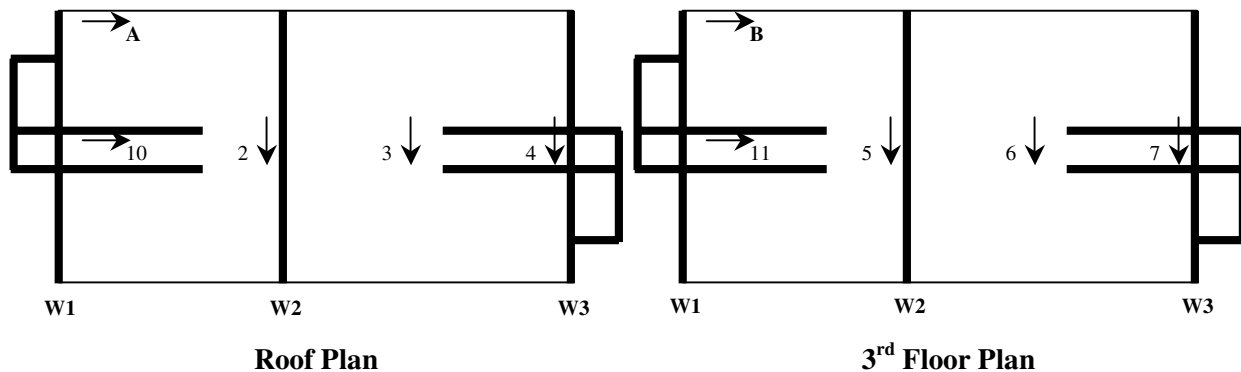


Figure 7. Locations for diaphragm flexibility verification, 3rd floor and roof diaphragms.

To compute the diaphragm flexibility ratio for the E-W direction, the maximum lateral deformation was assumed to occur near mid-span (sensor 3) between the supported ends of the sub-diaphragm at the north end. Therefore, taking the difference in displacement between sensor 3 and the average displacement at sensors 2 and 4 produced the maximum absolute displacement of the sub-diaphragm at the roof level. The drift of the vertical supporting elements was obtained by taking the difference between the drifts at the roof (sensor 2) minus the drift at the third floor (sensor 5). A similar procedure was used for the third floor taking the difference in displacement between sensor 6 and the average displacement at sensors 5 and 7 to obtain the maximum absolute displacement of the sub-diaphragm at the third level. The drift of the vertical supporting elements was obtained by taking the difference between the drifts at the third level (sensor 5) minus the drift at the second level sensor 8. It will be shown that the displacement response at sensor 4 is similar to sensor 2 and that sensor 7 is similar to sensor 5.

In the N-S direction, the sensors were located at the interior walls at the roof (10), 3rd floor (11) and 2nd floor (12) levels, corresponding instrumentation on the diaphragms was not available. Therefore locations directly opposite of locations 10 (Point A) at roof level and 11 (Point B) at the 3rd floor were used to calculate the relative displacement at the edge of the diaphragm. A procedure similar to that just discussed for the E-W direction was used to calculate the code displacement ratio.

Dynamic Loading

The predicted displacement response of the three-story building during the Landers earthquake was used to compute the code criteria for a flexible diaphragm at the roof and 3rd floor levels and in the N-S and E-W directions. In contrast to the static loading case, the dynamic loads were applied simultaneously to the structure as two acceleration time histories at the base in the N-S and E-W directions. Since the displacements varied with time, the displacement ratio was computed at the instant of maximum mid-span displacement in the diaphragm. After this initial calculation, the computations were identical to those performed for the static loading case.

Base Shear Distribution for E-W Shear Walls (Landers Earthquake)

To add further insight into the behavior of the diaphragms of the three-story building, dynamic time history results for the base shear were studied. It is well known that the distribution of lateral load to the vertical resisting elements depends upon the behavior of the diaphragm. If a diaphragm is perfectly rigid, the lateral resisting units (e.g. walls) will resist the lateral load in proportion to relative rigidities of the walls. In contrast, if the diaphragm is flexible, the lateral load is distributed in proportion to tributary area adjacent to the wall.

RESULTS

Diaphragm Flexibility

In this section, diaphragm flexibility verification is performed for the 3rd floor and roof diaphragms of the three-story building. Results shown reflect the use of static loading and dynamic loading to classify the flexibility of the diaphragms of the three-story building.

Static Loading

The deflected shape of the 3rd floor diaphragm of the three-story building subjected to inverted triangular lateral loading in the N-S and E-W directions is displayed in **Figure 8**. Similarly, **Figure 9** depicts the deflected shape of the roof diaphragm when loaded with the inverted triangular lateral load distribution. The calculated code displacement ratios for diaphragm flexibility in the N-S and E-W directions under static loading in the N-S and E-W directions are shown in **Table 2**, where values above 2.0 are representative of a flexible diaphragm.

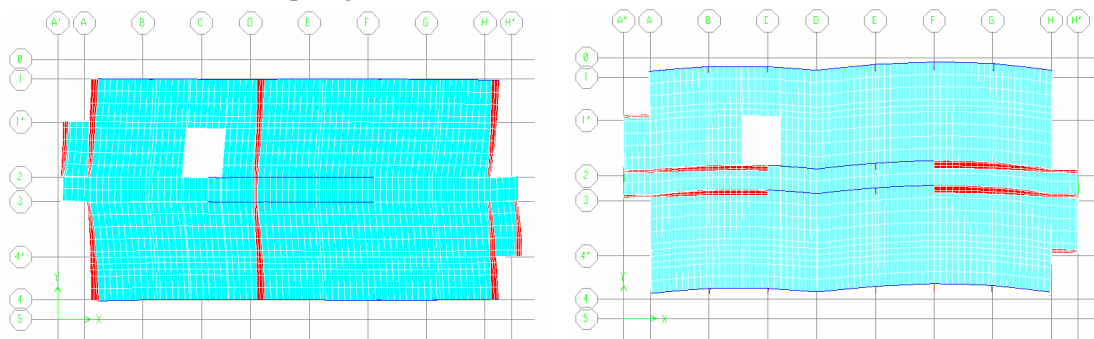


Figure 8. N-S and E-W deformed shape, '97 UBC static loads, 3rd floor.

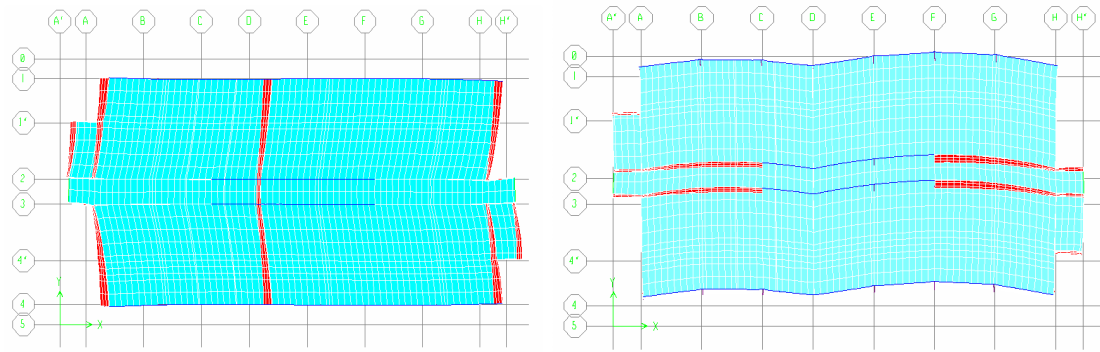


Figure 9. N-S and E-W deformed shape, '97 UBC static loads, roof.

Table 2. Diaphragm verification, '97 UBC static loading, roof & 3rd floor.

Static Loading				
Floor	Diaphragm orientation	Maximum diaphragm deformation	Corresponding average associated story drift	1997 UBC Code Ratio
		Δ_{max} (inches)	δ_0 (inches)	Δ_{max}/δ_0 (inch/inch)
Roof	E-W	0.1283	0.0255	5.03
	N-S	0.1384	0.0288	4.81
3rd	E-W	0.0788	0.0684	1.15
	N-S	0.0774	0.0576	1.34

**Note: Static loading in N-S and E-W directions applied separately

Dynamic Loading

Time history plots of the displacements relative to the base of the structure at the mid-span and support locations for the roof and 3rd floor diaphragms in the E-W direction as obtained using the ETABS mathematical model, are shown in **Figure 10**, and corresponding magnified views of the comparison for both diaphragms are shown in **Figure 11**. Additionally, **Figure 12** shows the variation of support displacement at walls W2 and W3, the supporting walls of the E-W diaphragm under consideration for the roof and 3rd floor diaphragms.

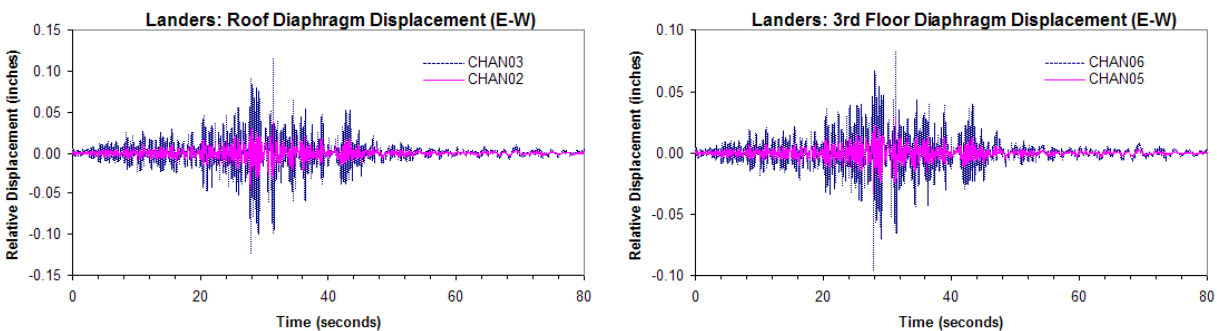


Figure 10. E-W midspan vs. support relative displacements, roof & 3rd floor.

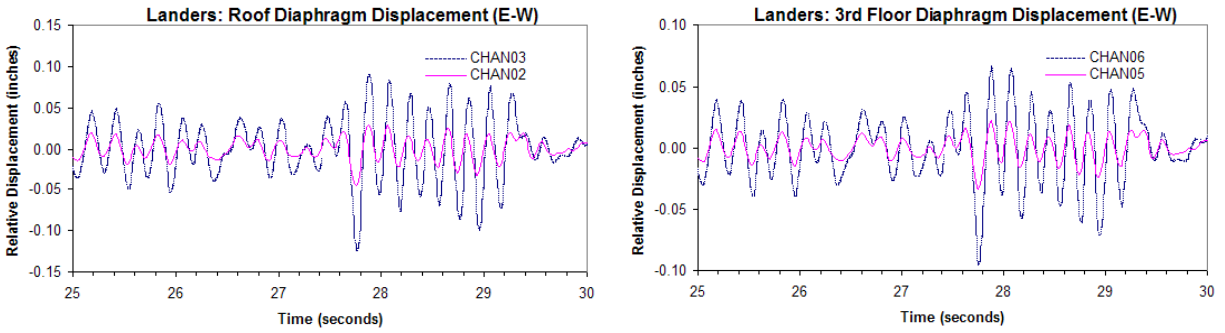


Figure 11. E-W midspan vs. support relative displacements (magnified), roof & 3rd floor.

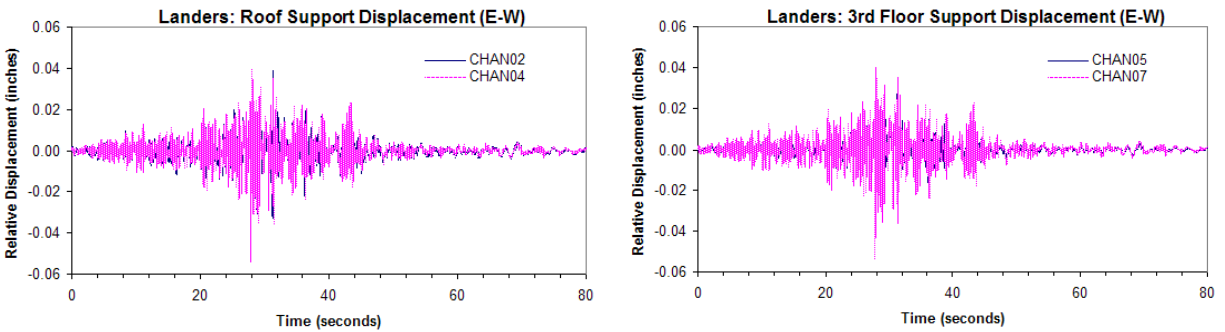


Figure 12. E-W supporting walls relative displacements, roof & 3rd floor.

The time history comparison of the relative displacement at sensor location 10 and point A on the roof diaphragm in the N-S direction are shown in **Figure 13**. A similar comparison for location 11 and point B for the 3rd floor diaphragm is also displayed in **Figure 13**, and the corresponding magnified views for the roof and 3rd floor diaphragms are shown in **Figure 14**. The results of the calculated flexibility ratios for the dynamic loading case are summarized in **Table 3**.

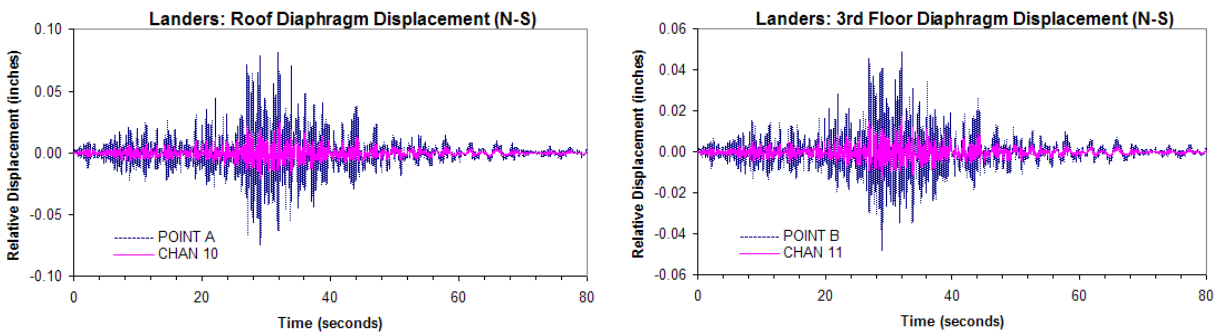


Figure 13. N-S midspan vs. support relative displacements, roof & 3rd floor.

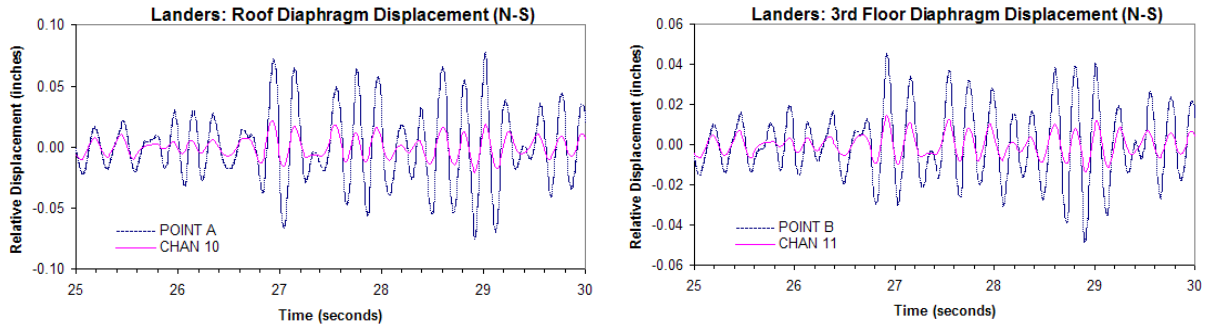


Figure 14. N-S midspan vs. support relative displacements (magnified), roof & 3rd floor.

Table 3. E-W and N-S diaphragm flexibility verification, dynamic loading, roof and 3rd floor diaphragms.

Dynamic Loading					
Floor	Diaphragm orientation	Maximum diaphragm deformation Δ_{max} (inches)	Time of maximum deformation t_{max} (seconds)	Corresponding average associated story drift δ_0 (inches)	1997 UBC Code Ratio Δ_{max}/δ_0 (inch/inch)
Roof	E-W	0.0807	31.28	0.0093	8.65
	N-S	0.0613	31.78	0.0071	8.66
3rd	E-W	-0.0619	27.76	-0.0159	3.90
	N-S	-0.0361	28.90	-0.0069	5.24

**Note: Dynamic loading in N-S and E-W directions applied simultaneously

Base Shear Distribution for E-W Shear Walls (Landers Earthquake)

A plot of the base shear in the supporting walls, W2 and W3, of the E-W diaphragm is shown in **Figure 15**. Likewise a comparison of the shear in walls W2 and W1 of the E-W diaphragm is also shown in **Figure 15**. **Figure 16** shows a comparison of the shear in walls W1 and W3. The base shears in the three main walls in the E-W direction under the Landers earthquake base motion are compared in **Figures 17 and 18** considering the actual flexibility of the diaphragms versus the use of a rigid diaphragm.

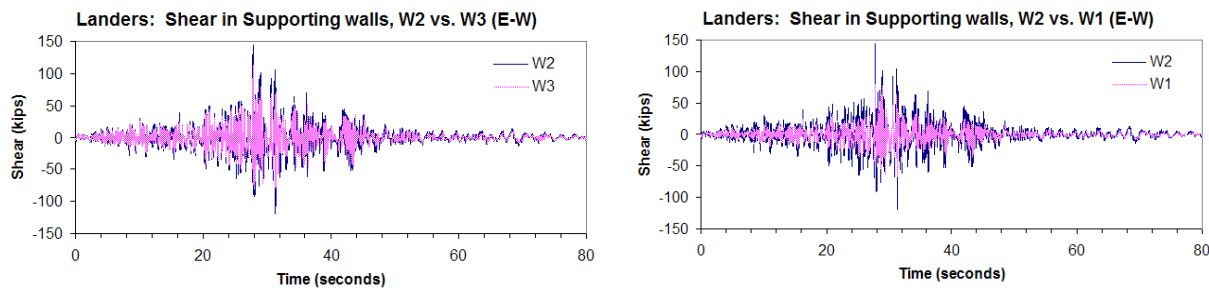


Figure 15. Base shear in E-W supporting walls, W2 vs. W3 & W2 vs. W1, Landers.

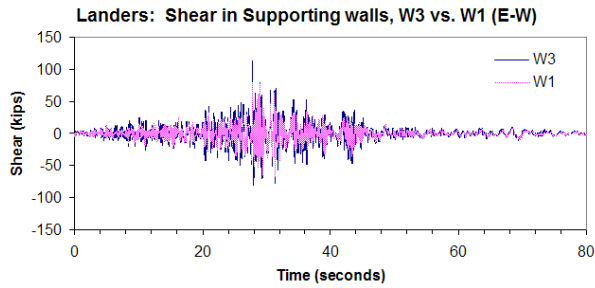


Figure 16. Base shear in E-W supporting walls W3 & W1, Landers.

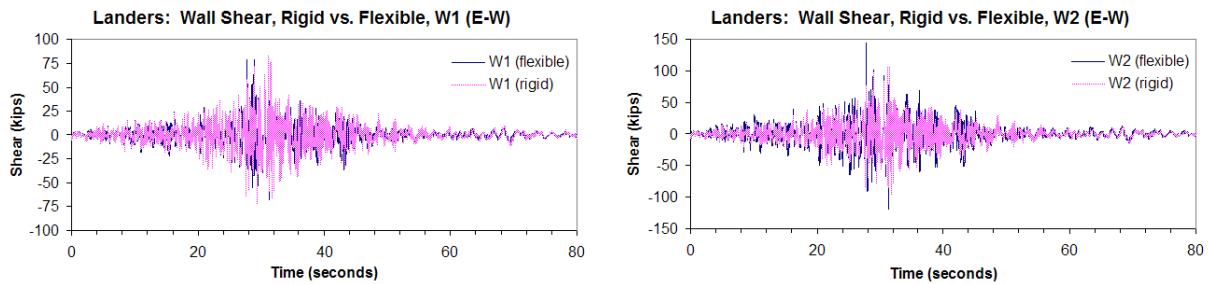


Figure 17. Base shear in supporting walls W1 (E-W) & W2 (E-W), rigid vs. flexible, Landers.

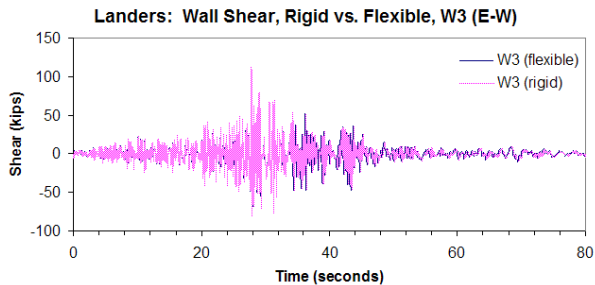


Figure 18. Base shear in supporting wall W3 (E-W), rigid vs. flexible, Landers.

DISCUSSION

Diaphragm Flexibility

Static Loading

Comparing the deflected roof and 3rd floor diaphragm in N-S direction in **Figures 8 and 9**, it can be seen that in the N-S direction, the diaphragm deforms as a cantilever off the two interior walls with the larger relative deformation occurring at the edge of the diaphragm at the roof level. Similarly, comparing **Figures 8 and 9** for the E-W direction indicates that the larger relative deformation in the E-W direction is also at the roof level and occurs near the center of each of the two sub-diaphragms.

The results of the comparisons in **Table 2** indicate that according to the aforementioned criteria, the roof diaphragm in both directions may be considered a flexible diaphragm. However, the third floor ratios are below 2.0 for both directions and may be considered as a rigid diaphragm.

Dynamic Loading

The magnified view showcasing the comparison of the midspan diaphragm displacement to the corresponding support relative displacements in the E-W direction in **Figure 11** show that the period of the oscillation of the displacement response is approximately 0.2 seconds, and is therefore in agreement with the fundamental period in the E-W direction obtained from the dynamic modal analyses. From **Figure 11** it is evident that the Roof and 3rd floor diaphragms in the E-W direction do not behave in a rigid manner, as the center of the diaphragm displaces substantially more than the supporting wall. From **Figures 12** it is clear that the two supporting walls undergo very similar displacements (which cause the graph to appear as if there is only one time history) for both the roof and 3rd floors.

For the N-S direction, from **Figure 14** it is seen that the magnified view of the diaphragm displacement time history comparison verifies that the period of the building in the N-S direction is approximately 0.2 seconds, as computed using modal analyses. Again, we see that even in the N-S direction, both the roof and 3rd floor diaphragms do not behave rigidly, as the “free” end displaces more than the supported end.

Table 3 indicates that the relative displacement ratios for both the roof and 3rd floor diaphragms exceed 2, thus implying that all the diaphragms in this building meet the 1997 UBC criteria for consideration as flexible diaphragms in both principal building directions. For the roof diaphragm, the results of the static and dynamic loading cases are similar, although the calculated ratios using dynamic loading are higher. However, the results for the 3rd floor diaphragm under dynamic loading are contradictory to those computed using static loads. The ratios for the 3rd floor diaphragm in both the N-S and E-W directions for the dynamic load case exceeded 2, indicating that this diaphragm also behaves in a flexible manner, in contrast to the result obtained under static load. More complete instrumentation is needed to evaluate the behavior of the diaphragm.

Base Shear Distribution for E-W Shear Walls (Landers Earthquake)

Figure 15 indicates that for generally all of the earthquake motion, the shear at the base of wall W2 is larger than for wall W3. At the time of maximum shear at the base of the middle wall, (27.76 seconds), the shear in wall W2 is 144 kips and the shear in end wall W3 at that time is 114 kips. Therefore, at this instant, the ratio of the shear in W2 to that in W3 is 1.27. Such a result suggests that the diaphragm in the E-W direction is behaving in a flexible manner. **Figure 15** also clearly indicates that wall W2 resists more shear than wall W1. At the point of maximum shear in wall W2 (144 kips), the corresponding shear in wall W1 is 71 kips, and thus the ratio of shear in wall W2 to wall W1 at this point is 2.0. Since the shear resisted by wall W2 is twice as much as the shear resisted in wall W1, it is likely that the E-W diaphragm behaves in a flexible manner. It is also interesting to note that the ratio of tributary areas W2/W1 is 2.33 and W2/W3 is 1.75. It should also be noted that part of this unbalance is due to the built-in eccentricity in the E-W direction. The effect of this eccentricity can also be seen in **Figure 16**.

The results determined from the study of base shear distribution is in general agreement with the results obtained using the code verification ratio for the dynamic loading case, where the behavior of both the roof and 3rd floor diaphragms in the E-W direction were found to be flexible. This result is also in agreement with the finding that under static loading in the E-W direction, the roof diaphragm behaves in a flexible manner, but this is not true for the 3rd floor diaphragm under similar loading.

The base shears in the wall (W1) at the south end of the building are shown in **Figure 17**. These results indicate that the maximum shears are about the same having values of 85 kips rigid vs. 80 kips flexible. At the middle wall (W2) the shear due to the actual diaphragm is 33% larger than that of the rigid diaphragm (143 kips vs. 107 kips) which is displayed in **Figure 17**. For wall W3 at the north end of the

building, the base shears are almost the same reaching 114 kips for the actual diaphragm compared to 108 kips for the rigid diaphragm as shown in **Figure 18**.

CONCLUSIONS

The three-story masonry building has recorded the response from three major earthquakes. However, due to the distance from the building to the epicenter of the earthquake, the base accelerations recorded at the building are relatively low with peak ground accelerations of between 4% and 7% of gravity. Spectral analyses of the recorded data indicate that the period of the fundamental translation modes in each direction are approximately 0.2 seconds. A similar result was obtained from the three dimensional ETABS model of the building. Moving window analyses of the recorded data indicate changes in period due to cracking but no permanent deformation.

However, using acceleration records obtained at stations closer to the epicenter of two recently recorded earthquakes, the results of the analyses indicate base shear values that far exceed the code minimums. Fortunately, the in-plane shear capacities of the designed walls in each principal direction have considerably higher strength than the code minimum requirements. These capacities are exceeded by the inertia forces developed in the walls under these stronger ground motions for only a limited number of cycles. This significantly higher capacity is due to the minimum steel requirements for structural walls.

From this investigation on the instrumented three-story building, it can be concluded that the criteria used in the building code for classifying a diaphragm as rigid or flexible contains considerable uncertainty. The value of the code displacement ratio depends upon the method used for the calculation. Significant differences were observed between the measured response obtained using static vs. dynamic loading. Calculated code ratios ranged between 0.73 and 2.55 for static loading, and between 2.1 and 3.8 for dynamic loading. Thus, when using dynamic loading, the code criteria classifies the roof and 3rd floor diaphragms in the N-S and E-W directions as flexible. However, using static loading, the resulting displacement ratios suggest that the roof diaphragm is flexible and the floor diaphragm is rigid. Consideration of base shear in the resisting walls also indicates the computed values are approximately proportional to the tributary area implying a flexible diaphragm.

REFERENCES

1. Abrams, D.P. "Response of Unreinforced Masonry Buildings." *Journal of Earthquake Engineering* 1997; 1(1): 257-273.
2. ICBO. "Uniform Building Code." Whittier, CA, 1997.
3. Tena-Colunga, A., Abrams, D.P. "Seismic Behavior of Structures with Flexible Diaphragms." *Journal of Structural Engineering* 1996; 122(4): 439-445.
4. CSMIP. "CSMIP Strong-Motion Records from the Northridge, California Earthquake of January 17, 1994." Report No. OSMS 94-07, California Dept of Conservation, Sacramento, CA, 1994.
5. Tokoro, K. "Seismic Performance of Two Instrumented Masonry Buildings." Master's Thesis, Department of Civil & Environmental Engineering, University of Southern California, Los Angeles, CA, 2002.
6. Computers and Structures, Inc. "ETABS Users Manual, Version 7.0." Computers and Structures, Inc., 1999.